Penetration depth and absorption mechanisms of spin currents in Ir 20 Mn 80 and Fe 50 Mn 50 polycrystalline films by ferromagnetic resonance and spin pumping

P. Merodio, A. Ghosh, C. Lemonias, E. Gautier, U. Ebels, M. Chshiev, H. Béa, Vincent Baltz, W. E. Bailey

Penetration depth and absorption mechanisms of spin currents in $Ir_{20}Mn_{80}$ and $Fe_{50}Mn_{50}$ polycrystalline films by ferromagnetic resonance and spin pumping

P. Merodio,[1] A. Ghosh,[1] C. Lemonias,[1] E. Gautier,[1] U. Ebels,[1] M. Chshiev,[1] H. Béa,[1,a)] V. Baltz,[1,a)] and W. E. Bailey[2,b)]
[1]*SPINTEC, UMR 8191 CNRS/INAC-CEA/UJF-Grenoble 1/Grenoble-INP, F-38054 Cedex, France*
[2]*Mat. Sci. and Engn. Program, Department of Appl. Phys. and Appl. Math., Columbia University, New York, New York 10027, USA*

(Received 20 November 2013; accepted 9 January 2014; published online 24 January 2014)

Spintronics relies on the spin dependent transport properties of ferromagnets (Fs). Although antiferromagnets (AFs) are used for their magnetic properties only, some fundamental F-spintronics phenomena like spin transfer torque, domain wall motion, and tunnel anisotropic magnetoresistance also occur with AFs, thus making AF-spintronics attractive. Here, room temperature critical depths and absorption mechanisms of spin currents in $Ir_{20}Mn_{80}$ and $Fe_{50}Mn_{50}$ are determined by F-resonance and spin pumping. In particular, we find room temperature critical depths originating from different absorption mechanisms: dephasing for $Ir_{20}Mn_{80}$ and spin flipping for $Fe_{50}Mn_{50}$. © *2014 AIP Publishing LLC*. [http://dx.doi.org/10.1063/1.4862971]

In the field of spintronics, the spin dependent transport properties of ferromagnets (Fs) lie at the heart of devices working principles, hence the terminology F-spintronics.[1] By way of contrast, antiferromagnets (AFs) have been used so far mostly for their magnetic properties: they pin the magnetization of an adjacent F via exchange bias in order to set the reference direction required for the spin of conduction electrons in spintronic devices.[2,3] However, AF-spintronics, i.e., spin dependent transport with AF, is now in its infancy,[4,5] and is identified as a significant exploratory topic in spintronics.[6–8] A first theoretical toy model showed spin transfer torque (STT) with F/AF bilayers and giant magnetoresistance (GMR) with AF spin valves.[9] For ideal AF crystals, STT is expected to act on a much longer length scale compared to F.[5] STT-switching of AFs would then require lower critical currents than STT-switching of Fs. This, together with the fact that the use of AFs suppresses stray fields, would result in lower device power consumption and ultimate downsize scalability. Although synthetic AFs (SAFs, i.e., two Fs coupled antiparallel usually by Ruderman-Kittel-Kasuya-Yosida interactions) are used to overcome device malfunction at reduced lateral dimensions associated with F stray fields (e.g., crosstalk in magnetic random access memories: mutual influence of neighboring cells supposed to be isolated one from another), SAFs never entirely compensate, and small, but non-zero stray fields persist. With AFs, the net compensation is intrinsic except for a very small part at the interface. The first theoretical model was soon followed by experimental evidence of AF-STT with currents injected in F/AF polycrystalline bilayers.[10] A growing number of studies have considered both theoretical and device aspects of AF-spintronics, including current-induced AF magnetic resonance[11,12] for radio-frequency components, AF domain wall motion,[13–17] experimental evidence of AF tunnel anisotropic magnetoresistance with in-plane[18,19] and out-of-plane[20] AF polycrystals, and tunnel magnetoresistance in artificial AF heterostructures[21] for memories and logic devices. Some of the critical parameters for spin dependent transport in general are: i) the spin penetration depth originating from different mechanisms like spin flip related to the terminology: spin diffusion length and spin precession dephasing with the associated spin dephasing length terminology, and ii) the spin mixing conductances, since they both control current perpendicular to plane GMR.[22] Magnetoresistive and dynamic experiments are the most common tools to study spin length scales and mixing conductances in thin films.[22] However, these two types of studies are not ideal for AF materials since the formerly shows very low magnetoresistive signals and the latter requires very high (THz) frequencies for dynamics excitation. An alternative way to determine spin absorption and spin mixing conductances in thin films was recently implemented. It is based on the spin pumping phenomenon, the STT reciprocal effect, and is best suited for AFs.[23–28] The method indirectly monitors spin absorption in materials surrounding a F_{res} layer excited at resonance by ferromagnetic resonance (FMR). The oscillating F_{res} magnetization transfers spin angular momentum to conduction electrons of the adjacent layers. Loss of spin angular momentum by the conduction electrons results in F_{res} resonance linewidth broadening. This latter is related to the attenuation (i.e., to the Gilbert damping α) of the F_{res} excitations. One can distinguish between local, i.e., intrinsic losses, i.e., inside the precessing F_{res} (α^0), and non-local, i.e., extrinsic damping where spins are lost outside the F_{res} (α^{pump}), i.e., absorbed by the surrounding materials/interfaces under study. For various materials/interfaces, this method compares the spin absorption efficiency (related to spin mixing conductances) since depending on the materials/interfaces properties the spins can be entirely absorbed or backscattered into the F_{res}. Additionally, this technique determines spin absorption

a)Electronic addresses: vincent.baltz@cea.fr and helene.bea@cea.fr
b)web54@columbia.edu

length scales by investigating the F_{res} damping variations with the thickness of the neighbouring spin sink (i.e., absorbing material under investigation).[27] In this paper, we study spin dependent transport in two typical AF polycrystalline thin films, IrMn and FeMn, using the spin pumping technique. We expect to measure the characteristic length scales and thereby to determine spin absorption mechanisms in these two materials.

In order to study spin dependent transport in two usual AF materials, NiFe(8)/Cu(3)/AF(t_{AF})/Al(2) (nm) heterostructures have been deposited at room temperature by dc-magnetron sputtering onto thermally oxidised 3×2 mm^2 silicon substrates.[3,28] The AFs with varying thicknesses t_{AF} are made from $Ir_{20}Mn_{80}$ and $Fe_{50}Mn_{50}$ targets, respectively. The F_{res} NiFe(8) layer is deposited from a $Ni_{20}Fe_{80}$ target. The Al(2) cap oxidizes in air and consequently forms an AlOx protecting film with a low spin current absorption.[28] The Cu(3) breaks the F/AF direct magnetic exchange interactions, evidenced through negligible hysteresis loop shifts measured by vibrating sample magnetometry (VSM) at 300 and 4 K (not shown). In addition, given that Cu(3) is a light element and since its spin diffusion length is much longer than its 3 nm thickness,[22] it does not alter spin propagation between the F and the AF.

Figure 1 illustrates the FMR measurement configuration and principle. The local magnetization ($\boldsymbol{m}(t)$) of the NiFe is excited to resonance by a small RF pumping magnetic field (H_{RF}). As a consequence, the NiFe generates a pure spin current (I_S^{pump}) when oscillating around the local effective field (H^{eff}) due to the spin pumping effect. This spin current diffuses through the NiFe/Cu/AF trilayers and concurrently transfers spin angular momentum to the conduction electrons. It is so to say absorbed or reflected at interfaces and within layers due to spin dependent scattering and in return it affects the NiFe Gilbert damping: $\alpha = \alpha^0 + \alpha^{pump}$, where α^0 is the local intrinsic F damping and α^{pump} is the extra non-local damping. In the figure, λ_{AF} denotes the critical absorption depth over which the coherence of the spin current within the AF is lost. Consequently the extra F damping due to the AF levels out above λ_{AF}.[28] The NiFe total Gilbert damping (α) is extracted from series of F resonance spectra obtained with a broadband coplanar waveguide. In-plane DC bias magnetic field (H_{DC}) is employed. A small 2 to 20 Oe modulation field of 201 Hz is applied along the DC field for lock-in detection of the transmitted signal to improve sensitivity and excitation frequencies ($\omega/2\pi$) ranging between 2 and 20 GHz are used. For each frequency the resonance linewidth is determined by fitting the resonance spectra (differential power absorption vs H_{DC}) to a Lorenzian derivative. The total Gilbert damping α is extracted from: $\Delta H_{pp}(\omega) = \Delta H_0 + \frac{2}{\sqrt{3}}\alpha\omega/|\gamma|$, where ΔH_{pp} is the peak-to-peak linewidth of the Lorenzian derivative fit, γ the gyromagnetic ratio, and ΔH_0 the inhomogeneous broadening associated with spatial variations in the magnitude of the out-of-plane magnetic anisotropy. A linewidth versus $\omega/2\pi$ plots and a representative spectrum are shown Fig. 2. For the various NiFe(8)/Cu(3)/AF(t_{AF})/Al(2) (nm) heterostructures, non-local damping α^{pump} ascribed to absorption of spin angular momentum by the AF only is straightforwardly obtained by subtracting the corresponding total Gilbert damping from the total Gilbert damping obtained for $t_{AF} = 0$.

Figure 3 shows α^{pump} vs t_{AF} for IrMn and FeMn. For some t_{AF}, either the same sample is measured twice or two samples of the same composition are deposited and measured. The maximum difference is observed for $t_{FeMn} = 15$ nm and defines the error bars of $\sim 1.4\times10^{-4}$. We observe that, α^{pump} increases linearly with t_{IrMn} and cuts off to a maximum at an empirical critical thickness $\lambda_{IrMn}/2$ of around 1.4 nm. Like in Ref. 24, we consider that the spins relax on the way forward in the IrMn depth, reflect and return backward through the IrMn to the NiFe layer, thus traversing and relaxing linearly twice in the IrMn depth. The linear behaviour is similar to F spin sinks,[28,29] indicating that the nature of the absorption for IrMn mainly relates to dephasing of the spin current transverse component as well: the spins undergo Larmor precession as they go into the material because the majority and minority Fermi wave vectors are different. Spins with different initial conditions precess at different rates, leading to classical dephasing. Given that, λ_{IrMn} is mostly related to spin dephasing proportional to the integration over the Fermi wave vectors of $\pi/|k_f^{\uparrow}\text{-}k_f^{\downarrow}|$ where $k_f^{\uparrow(\downarrow)}$ are the majority (minority) Fermi wave vectors, or equivalently

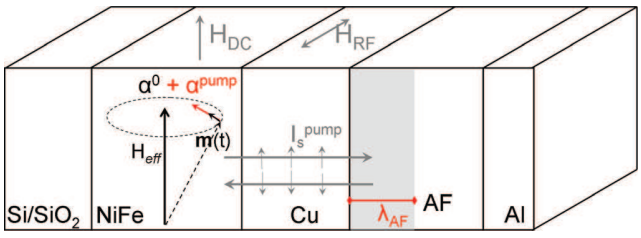

FIG. 1. Scheme illustrating the phenomenon for our Si/SiO_2//NiFe/Cu/AF/Al stacks with AF = IrMn or FeMn. A precession of the NiFe magnetization around the effective magnetic field (H_{eff}) is initiated by application of an external RF field (H_{RF}) under a given static DC field (H_{DC}). Relaxation of the NiFe magnetization along H_{eff} originates from two main sources: the intrinsic damping inherent to the NiFe layer (α^0) and the damping due to the spin current generated by the F excitations then diffused through the multilayer and finally pumped/reflected by the AF (α^{pump}). Beyond a critical length (λ_{AF}) characteristic of the spin dependent transport in the AF, the coherence of the spin current in the AF is lost.

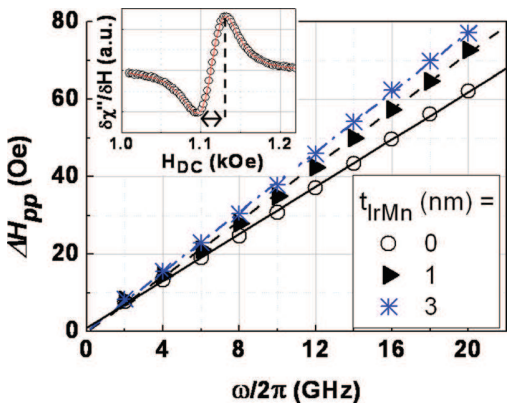

FIG. 2. Dependence of the resonance linewidth (ΔH_{pp}) with the excitation frequencies ($\omega/2\pi$) for Si/SiO_2//NiFe(8)/Cu(3)/IrMn(t_{IrMn})/Al(2) (nm) stacks with $t_{IrMn} = 0$, 1, and 3 nm. The lines are linear fit to the data. Inset: typical resonance spectrum, i.e. differential power absorption ($\delta\chi''/\delta H$) vs DC bias field (H_{DC}) for $t_{IrMn} = 1$ nm and $(\omega/2\pi) = 10$ GHz; the peak-to-peak linewidth gives ΔH_{pp} and is indicated by the arrow.

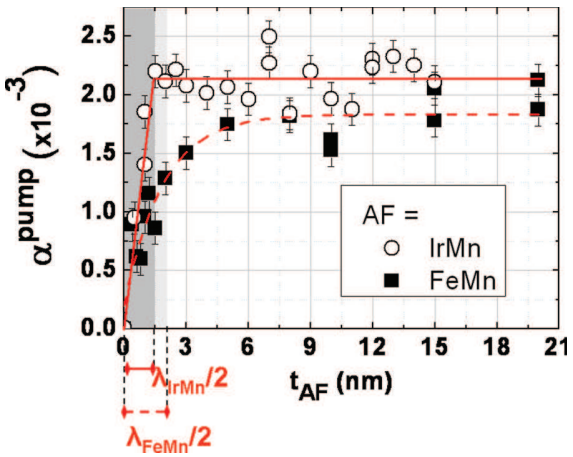

FIG. 3. Dependence with t_{AF} of the AF contribution, via spin pumping, to the NiFe magnetization damping (α^{pump}) for Si/SiO_2//NiFe(8)/Cu(3)/AF(t_{AF})/Al(2) (nm) stacks with various AF thicknesses (t_{AF}) and AF = IrMn and FeMn. For IrMn, the straight line is a linear fit proportional to: $2t_{IrMn}/\lambda_{IrMn}$ for $t_{IrMn} < 1.4$ nm and a guide to the eye above. For FeMn, the dashed line is an exponential fit of the form: $A.[1-\exp(-2t_{FeMn}/\lambda_{FeMn})]$. The spin dependent transport characteristic length in the AF is λ_{AF}.

$hv_g/2\Delta_{ex}$, with v_g the spin-averaged group velocity and Δ_{ex} the exchange splitting. Δ_{ex} is smaller for IrMn compared with the usual F due to a low critical order temperature T_N of around 350–400 °C.[30] Because of that we were expecting that λ_{IrMn} should be even larger than the critical lengths of usual Fs: CoFeB, Co or NiFe for which $\lambda_F/2 \sim 1.2$ nm.[28,31] Although the linear behaviour of α^{pump} vs t_{IrMn} clearly points out spin dephasing mechanism as the main source of absorption, the fact that Ir is a heavy element and carries *d* electrons in the conduction band, probably introduces to a less extent some additional spin flip mechanisms balancing the effect of lower Δ_{ex} and contributing to slightly reducing the characteristic penetration length to a value similar to that of usual Fs. From Fig. 3, we observe that the α^{pump} vs t_{FeMn} follows a totally different trend with an exponential $[1\text{-}\exp(-2t_{FeMn}/\lambda_{FeMn})]$ thickness dependence. Such a trend is typical of a paramagnetic spin sink for which the absorption of the spin current is in contrast mainly due to spin flipping.[24,27] For consistency, we also consider here the empirical factor 2[24] taking into account the forward and backward path of spins within the FeMn layer. Fits of the raw data with the above exponential law give a $\lambda_{FeMn}/2$ of around 1.9 nm. In this case, λ_{FeMn} relates to spin diffusion in contrast to λ_{IrMn} originating from spin dephasing, although practically both give values proportional to critical spin penetration depths. Given that, λ_{IrMn} concerns the spin transverse component absorption when λ_{FeMn} is associated to both longitudinal and transverse components absorptions. Such paramagnetic α^{pump} vs t_{FeMn} variations at room-T are the consequence of the low exchange splitting Δ_{ex} of FeMn.[2,31] It is not unlikely that, at room-T FeMn films thinner than λ_{FeMn} are paramagnetic rather than antiferromagnetic given the reduced bulk T_N of FeMn compared to IrMn[2] to which adds finite size effects additionally reducing T_N.[30,32] Accurately measuring and estimating finite size effects on T_N is not simple and very few corresponding literature is available for AF materials. A toy model in Ref. 32 reproduces finite size effects on F layers critical temperature. The model is transferable to AFs[33] and gives the following general power law: $T_N(n) = T_N(bulk)\cdot\{1\text{-}[(N_0+1)/(2n)]^k\}$, where n is the number of AF monolayers (ML), N_0 the AF exchange length, and k an integer. For 3D Ising models, k is close to 1.6. Conversely, accurate values of N_0 are not straightforwardly accessible to experiments and models. Alternatively, T_N is accessible to experiments via ultrafast measurements of F/AF exchange bias bilayers. The blocking temperature (T_B) is the temperature above which the F is no longer pinned in a fixed direction by the AF. It depends on various parameters among which the F/AF interfacial coupling, the AF bulk properties (AF-AF exchange stiffness and grain volume) and time. In particular, T_B increases with the F magnetization sweep-rate and reaches the AF intrinsic critical Néel-T (T_N) in the nanosecond regime.[30] Reference 30 is to our knowledge the only paper dealing with that: for 30 ns pulses, the critical T for IrMn reduces from 350–400 °C (i.e., bulk value) for 6.5 nm to 200 °C for 4.5 nm. In the case of FeMn, the same authors measure a reduction from 200 °C (i.e., bulk value) for 7 nm to 100 °C for 5 nm. Such measurements are compatible with T_N lower than room-temperature for few nm thick FeMn.

Figure 3 also shows that for both IrMn and FeMn layers, α^{pump} levels out for thick AF. The α^{pump} saturation value (α^{pump}_{sat}), i.e., after maximum spin absorption, seems to be slightly larger for IrMn. Given the above mentioned distinct behaviours for IrMn and FeMn, α^{pump}_{sat} originates from the corresponding distinct mechanisms. For the paramagnetic-like FeMn, α^{pump}_{sat} is mostly related to spin flipping that is bulk-like. In contrast, for the F-like IrMn, α^{pump}_{sat} mostly relates to the effective spin mixing conductance ($g^{\uparrow\downarrow}_{eff}$) that mostly depends on the Cu/IrMn interface ($g^{\uparrow\downarrow}_{Cu/IrMn}$) since the values of α^{pump} reported in this study result from the difference between the damping for NiFe(8)/Cu(3)/AF(t_{AF})/Al(2) and NiFe(8)/Cu(3)/Al(2) (nm). As described in Ref. 28, the measured values of effective spin mixing conductance from the addition of the AF layer do not depend on the spin mixing conductance of NiFe/Cu ($g^{\uparrow\downarrow}_{NiFe/Cu}/S \sim 14.4 +/- 1.4\,nm^{-2}$), which cancels due to the Cu Sharvin conductance correction of the same order of magnitude. In addition, to a first approximation, given that the AF randomizes spins over short distances, the Cu/AF interface mainly drives spin mixing. If the uncompensated spins at the AF interface were fully oriented toward the same direction, we would expect Cu/IrMn spin pumping conductivity ($g^{\uparrow\downarrow}_{Cu/IrMn}/S$) similar to Cu/F, typically around 14 to 16 nm^{-2}. However AF interfaces are known to be highly frustrated,[34,35] and the resulting overall picture gives few uncompensated spins (e.g., tiny F regions) at the AF interface, also responsible for exchange bias. While an AF spin surface in contact with an F is tuned by the interfacial F spin configuration that orients the AF uncompensated spins in a preferential direction after field cooling, in the present case of Cu/AF the AF interfacial uncompensated spins are rather randomly oriented positively and negatively. Therefore, the influence of the uncompensated AF interfacial spins on the Cu/AF spin mixing conductance is hard to anticipate here. Finally, note that the Cu/IrMn interface is surely more complex due to the formation of CuMn spin-glasses.[35–37]

To conclude, in the context of AF-spintronics, the main contribution of the present study is the determination of

room temperature critical penetration depths and absorption mechanisms of spin currents in $Ir_{20}Mn_{80}$ and $Fe_{50}Mn_{50}$ spin sinks by means of F-resonance and spin pumping. Different room temperature absorption mechanisms of spins were evidenced: dephasing for IrMn and spin flipping for FeMn probably due to the room temperature paramagnetic character of FeMn for thicknesses lower than the penetration depth. Future works could involve other AFs and variable temperature for studies of the para- to antiferro-magnetic transition temperature: difficult to determine by many other techniques.

[1]S. A. Wolf, D. D. Awschalom, R. A. Buhrman, J. M. Daughton, S. von Molna, M. L. Roukes, A. Y. Chtchelkanova, and D. M. Treger, Science **294**, 1488 (2001).
[2]J. Nogués and I. K. Schuller, J. Magn. Magn. Mater. **192**, 203 (1999).
[3]V. Baltz, B. Rodmacq, A. Zarefy, L. Lechevallier, and B. Dieny, Phys. Rev. B **81**, 052404 (2010).
[4]J. Bass, A. Sharma, Z. Wei, and M. Tsoi, J. Magn. **13**, 1 (2008).
[5]A. H. MacDonald and M. Tsoi, Philos. Trans. R. Soc. **369**, 3098 (2011).
[6]R. Duine, Nat. Mater. **10**, 344 (2011).
[7]J. Sinova and I. Žutić, Nat. Mater. **11**, 368 (2012).
[8]A. Brataas, A. D. Kent, and H. Ohno, Nat. Mater. **11**, 372 (2012).
[9]A. S. Núñez, R. A. Duine, P. Haney, and A. H. MacDonald, Phys. Rev. B **73**, 214426 (2006).
[10]Z. Wei, A. Sharma, A. Núñez, P. M. Haney, R. A. Duine, J. Bass, A. H. MacDonald, and M. Tsoi, Phys. Rev. Lett. **98**, 116603 (2007).
[11]H. V. Gomoney, R. V. Kunitsyn, and V. M. Loktev, Phys. Rev. B **85**, 134446 (2012).
[12]Yu. V. Gulyaev, P. E. Zil'berman, and E. M. Epshtein, Radiotekhnika Elektronika **57**, 558 (2012).
[13]A. Manchon, N. Ryzhanova, A. Vedyayev, and B. Dieny, J. Appl. Phys. **103**, 07A721 (2008).
[14]R. Wieser, E. Y. Vedmedenko, and R. Wiesendanger, Phys. Rev. Lett. **106**, 067204 (2011).
[15]K. M. D. Hals, Y. Tserkovnyak, and A. Brataas, Phys. Rev. Lett. **106**, 107206 (2011).
[16]A. C. Swaving and R. A. Duine, Phys. Rev. B **83**, 054428 (2011).
[17]J. M. Logan, H. C. Kim, D. Rosenmann, Z. Cai, R. Divan, O. G. Shpyrko, and E. D. Isaacs, Appl. Phys. Lett. **100**, 192405 (2012).
[18]B. G. Park, J. Wunderlich, X. Martí, V. Holý, Y. Kurosaki, M. Yamada, H. Yamamoto, A. Nishide, J. Hayakawa, H. Takahashi, A. B. Shick, and T. Jungwirth, Nat. Mater. **10**, 347 (2011).
[19]D. Petti, E. Albisetti, H. Reichlová, J. Gazquez, M. Varela, M. Molina-Ruiz, A. F. Lopeandía, K. Olejník, V. Novák, I. Fina, B. Dkhil, J. Hayakawa, X. Marti, J. Wunderlich, T. Jungwirth, and R. Bertacco, Appl. Phys. Lett. **102**, 192404 (2013).
[20]Y. Y. Wang, C. Song, B. Cui, G. Y. Wang, F. Zeng, and F. Pan, Phys. Rev. Lett. **109**, 137201 (2012).
[21]P. Bose, I. Mertig, and J. Henk, Phys. Rev. B **75**, 100402 (2007).
[22]J. Bass and W. P. Pratt, Jr., J. Phys.: Condens. Matter **19**, 183201 (2007).
[23]L. Berger, Phys. Rev. B **54**, 9353 (1996).
[24]J. Foros, G. Woltersdorf, B. Heinrich, and A. Brataas, J. Appl. Phys. **97**, 10A714 (2005).
[25]Y. Tserkovnyak, A. Brataas, and G. E. W. Bauer, Phys. Rev. Lett. **88**, 117601 (2002).
[26]B. Heinrich, Y. Tserkovnyak, G. Woltersdorf, A. Brataas, R. Urban, and G. E. W. Bauer, Phys. Rev. Lett. **90**, 187601 (2003).
[27]S. Mizukami, Y. Ando, and T. Miyazaki, Jpn. J. Appl. Phys. **40**, 580 (2001).
[28]A. Ghosh, S. Auffret, U. Ebels, and W. E. Bailey, Phys. Rev. Lett. **109**, 127202 (2012).
[29]K. Carva and I. Turek, Phys. Rev. B **76**, 104409 (2007).
[30]L. Lombard, E. Gapihan, R. C. Sousa, Y. Dahmane, Y. Conraux, C. Portemont, C. Ducruet, C. Papusoi, I. L. Prejbeanu, J. P. Nozières, B. Dieny, and A. Schuhl, J. Appl. Phys. **107**, 09D728 (2010).
[31]W. E. Bailey, A. Ghosh, S. Auffret, E. Gautier, U. Ebels, F. Wilhelm, and A. Rogalev, Phys. Rev. B **86**, 144403 (2012).
[32]R. Zhang and R. F. Willis, Phys. Rev. Lett. **86**, 2665 (2001).
[33]T. Ambrose and C. L. Chien, Phys. Rev. Lett. **76**, 1743 (1996).
[34]K. Takano, R. H. Kodama, A. E. Berkowitz, W. Cao, and G. Thomas, Phys. Rev. Lett. **79**, 1130 (1997).
[35]K. Akmaldinov, S. Auffret, I. Joumard, B. Dieny, and V. Baltz, Appl. Phys. Lett. **103**, 042415 (2013).
[36]P. Gibbs, T. M. Harden, and J. H. Smith, J. Phys. F: Met. Phys. **15**, 213 (1985).
[37]R. K. Chouhan and A. Mookerjee, J. Magn. Magn. Mater. **323**, 868 (2011).